Journal of Non-Crystalline Solids: X 3 (2019) 100028

Contents lists available at ScienceDirect

Journal of Non-Crystalline Solids: X

journal homepage: www.journals.elsevier.com/journal-of-non-crystalline-solids-x

Topological constraint model of high lithium content borate glasses

Wataru Takeda[a], Collin J. Wilkinson[b], Steven A. Feller[a,*], John C. Mauro[b]

[a] Physics Department, Coe College, Cedar Rapids, IA 52402, USA
[b] Department of Materials Science and Engineering, The Pennsylvania State University, University Park, PA 16802, USA

ARTICLE INFO

Keywords:
Borate
Structure
Topological constraint theory
Conductivity
T_g
Modeling

ABSTRACT

Lithium borate glasses exhibit the “boron anomaly” and clustering of the lithium ions. Bødker et.al (Bødker, Mauro, Youngman, & Smedskjaer, 2019) predicted the Tg using statistical mechanics and topological constraint theory (TCT) over a wide range of contents (to 65 mol% Li_2O). Although Bødker's model predicted the fraction of the structures present, this paper examines the linkage between intermediate-range structures and properties of the glasses. Tg was found using TCT with the structural model of Feller, Dell, and Bray (Feller, Dell, Bray, 1982). The topology of the intermediate-range structure was related to rigidity, and to lithium clustering.

1. Introduction

Lithium borate glasses undergo complicated structural evolutions in the network as more modifier is added. Even though ample studies have been performed (NMR, Raman spectroscopy, infrared spectroscopy, MD simulation, etc.) [1–4], there is limited knowledge of how structure affects the properties of borate glass systems. In 2009, Mauro et al. [5] showed an analysis of $xM_2O\cdot(1\text{-}x)B_2O_3$ by applying the Mauro-Gupta topological constraint theory (TCT), where M is the alkali modifier, to predict fragility and the glass transition temperature (T_g) in a narrow region of lithium oxide concentrations ($0 \le x \le 0.4$). It was the first study which showed a direct quantitative connection between a compositional dependent structural model (the random pair model by Gupta [6]) and the properties of glasses. Recently, Bødker et al. [7] successfully predicted the T_g over a wider range of lithium oxide concentration ($0 \le x \le 0.65$) by applying the structural model derived from statistical mechanics using the empirical structural model by Feller et al. [8] to TCT. Although Bødker's model successfully modified the Feller model by statistically calculating the relative enthalpic contribution to the structural evolutions by using Mauro's statistical model [9], more in-depth analysis of the connection between structural properties and the properties of the glasses must be developed. To understand the structural properties of lithium borate glasses over this wide range of composition ($0 \le x \le 0.65$), further TCT modeling was implemented to analyze the lithium borate glass systems by calculating T_g. In order to ease the structural calculations, we use R for the molar ratio of lithium oxide to boron oxide defined as,

$$R = \frac{x}{1-x}. \tag{1}$$

Lithium borate glasses change structure as lithium oxide is added in the systems. Structure changes at both short- and intermediate-range level. Also, there are known clustering effects [2] of the lithium ions; due to this it is necessary to create other structural models of these systems. This study shows that TCT, when considering alkali clustering, is able to calculate the ionic properties of the glasses accurately. We will compare ionic conductivity with the number of constraints in the lithium borate glasses.

2. Mauro-Gupta topological constraint theory (TCT)

TCT is capable of predicting T_g based on the coordination of the glass forming atoms by using the relationship shown below [5,10],

$$\frac{T_g(R)}{T_g(R_r)} = \frac{S_c[T_g(R_r), R_r]}{S_c[T_g(R), R]}, \tag{2}$$

where S_c is the configurational entropy, and R_r is the reference composition. According to the energy landscape modeling of Naumis [11,12] the configurational entropy of a system is largely proportional to the number of low-frequency modes (atomic degrees of freedom), $f[T_g(R), R]$. At temperature $T_g(R)$, Eq. (2) may be rewritten as

$$\frac{T_g(R)}{T_g(R_r)} = \frac{f[T_g(R_r), R_r]}{f[T_g(R), R]} = \frac{d - n[T_g(R_r), R_r]}{d - n[T_g(R), R]}, \tag{3}$$

where $d = 3$ is the dimensionality of the network and $n[T, R]$ is the function of the average number of constraints per atom [5,10].

---

[*] Corresponding author.
E-mail address: sfeller@coe.edu (S.A. Feller).

https://doi.org/10.1016/j.nocx.2019.100028
Received 25 February 2019; Received in revised form 31 May 2019

The average constraints per atom in a network can be calculated averaging over all network forming species *i* and each type of constraint λ, where λ are the various constraints including two-body linear, bending angles and torsional angular or higher order constraints. Here, the network forming species are defined as the atoms which bond with more than two other atoms to form a continuous network. We define $N_i(R)$ as the mole fraction of network forming species at composition *R*. Therefore, the average number of constraints, $n[T,R]$, in atoms can be expressed as

$$n[T,R] = \sum_i N_i(R) \sum w_{i,}q(T), \tag{4}$$

where $w_{i,\lambda}$ is the number of λ-type constraints associated with network forming species *i*, and the temperature dependence of constraints is $q_\lambda(T)$, which measure the rigidity of each constraint λ [13,14]. In this study, we use the discrete form of the temperature dependence constraints, $q_\lambda(T)$. The limiting conditions of $q_\lambda(T)$ are

$$\lim_{T\to 0} q(T) = 1,\ \lim_{T\to\infty} q(T) = 0, \tag{5}$$

and the step is considered to be discontinuous at the onset temperature.

The following constraints are taken into consideration:

- α: B—O linear constraints: linear constraints are counted on each bridging oxygen.
- β: O-B-O angular constraints: there are five β constraints per tetrahedral boron and three β constraints per trigonal boron.
- μ: additional modifier rigidity due to clustering effects [2], two rigid μ constraints per lithium ion which contributes to form a network.
- γ: B-O-B, B-O-M* angular constraints: M* is a modifier cation which makes μ *constraints.* There is one γ constraint at these kinds of oxygen.

The constraint onset temperatures are ordered such that

$$T_\gamma < T_g(0) < T_\beta < T_\mu < T_\alpha. \tag{6}$$

3. Model

Pure B_2O_3 glass (*R* = *0*) consists of trigonal borons with three bridging oxygens [1]. When a modifier is added to B_2O_3, there are two possible short-range structure changes:

- Creation of non-bridging oxygen in three-coordinated borons.
- Converting the coordination of boron from three-coordination to four-coordination with a negative charge; there are no non-bridging oxygens in four-coordinated boron.

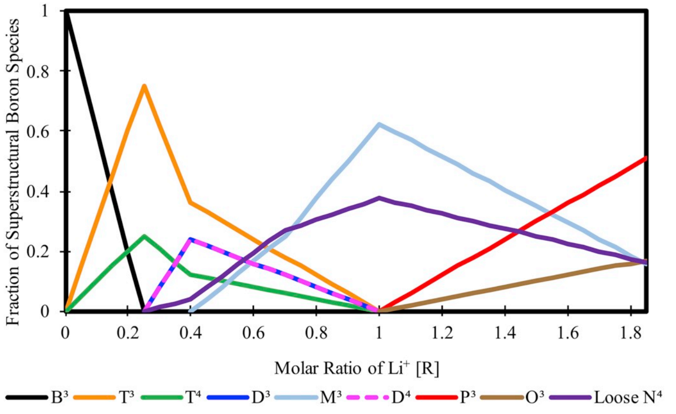

Fig. 1. Model of structural groups of lithium borate glass systems. B, T, D, Loose N^4, M, P and O are fractions of short and intermediate range structures. B = boroxol rings, T = tetraborate units, D = diborate units, loose N^4 = loose tetrahedra, M = metaborate units, P = pyroborate units and O = isolated orthoborate triangles. The superscripts 3 and 4 represent coordination numbers of boron in each of the units.

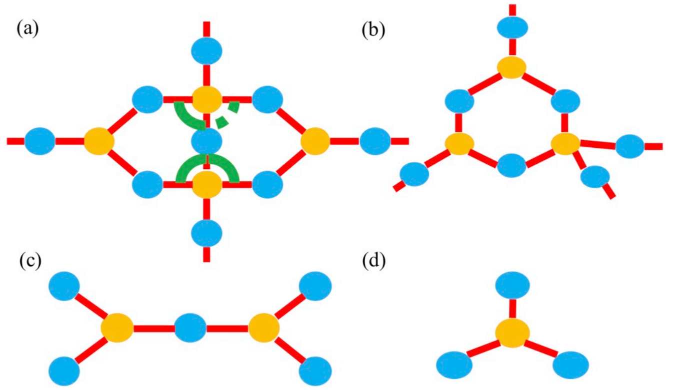

Fig. 2. Blue circles represents oxygen atoms and orange circles represents boron atoms. (a) represents diborate ring has two four coordinated borons (D^4) and two three coordinated borons (D^3). (a) shows that arbitrary three of four angles (shown in green colour) associated with D^4 must be specified, one angle (shown as dotted) is already determined. (b) represents triborate ring with two T^3 and one T^4. (c) is the combination of three-coordinated boron with two NBOs (P^3), namely pyroborate. (d) is three-coordinated boron with three NBOs (O^3), namely orthoborate. (For interpretation of the references to colour in this figure legend, the reader is referred to the web version of this article.)

Krogh-Moe proposed that $RM_2O{\cdot}B_2O_3$ glass systems are constructed from intermediate-range structures called superstructural groups. There are boroxol, tetraborate, diborate, metaborate, pyroborate, orthoborate and "loose" four-coordinated boron which are not part of any superstructural groups [3]. These compositional dependent structural evolutions of borate glasses have been studied by both theoretical and empirical means. The algebraic theory of the random pair model of Gupta [6], has accurately predicted the fraction of four-coordinated boron in alkali borate systems over a wide range of compositions. However, the random pair model does not show the evolution of superstructural groups. Thus, we use the empirical structural models of $RM_2O{\cdot}B_2O_3$ systems based on NMR studies by Jellison, Bray, Dell, Yun and Feller, which is able to compute the fraction of superstructural groups in the region ($0 \le R \le 1.86$) [1,8]. We chose Feller model as a representative one using NMR data [8]. Following Feller model, we set the expressions for each four-coordinated boron and three-coordinated boron associated with each superstructural groups. T^4 denotes the fraction of all four-coordinated borons in tetraborate in the glasses, B^3 is the fraction of all three-coordinated borons in boroxol, D^4 is the fraction of all four-coordinated borons in diborate, loose N^4 is the fraction of "loose" four-coordinated borons etc., where the superscripts illustrate whether each borons are four-coordinated or three-coordinated (shown in Fig. 1 and Fig. 2). A large unit, such as the superstructural group, may cause overcounted constraints [15]. For example, β constraints could be overcounted in the diborate rings (shown in Fig. 2(a)). The diborate ring has two D^4 units bonded with a bridging oxygen in the middle. One might consider five β constraints in D^4 in the diborate ring. However, one of the four angles of the inner side of the tetrahedron is always fixed, and therefore, need not be counted as a β constraint [15]. β constraints in D^4 should be counted as 4.5, as shown in the following equation,

$$\beta_{D^4} = \frac{Number\ of\ \beta\ constraints\ in\ Diborate}{Number\ of\ tetrahedra\ in\ Diborate\ (D^4)} = \frac{9}{2} = 4.5. \tag{7}$$

We suggest that there are five network-forming species to consider in this system as listed below,

- B^{4*}: Four-coordinated boron which includes T^4 and *Loose* N^4.

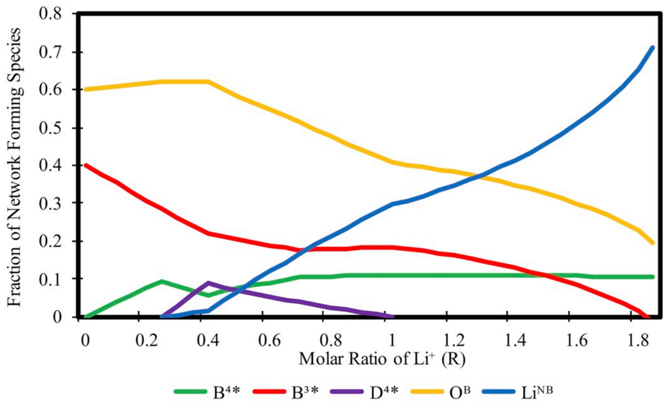

Fig. 3. Fraction of network forming species following Eqs. (9.a)–(9.e).

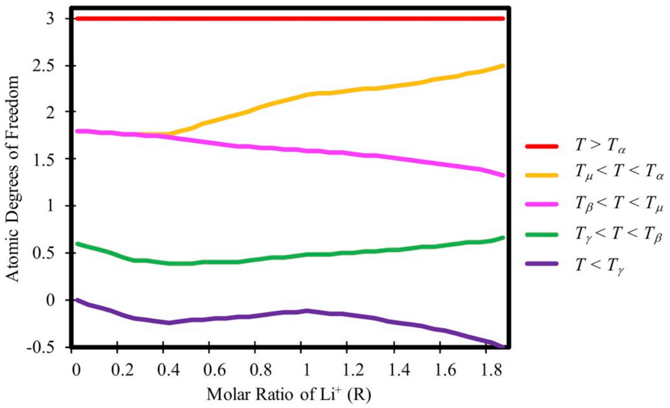

Fig. 4. Temperature and composition dependence of the average number of atomic degrees of freedom in the lithium borate glass systems. T_α, T_μ, T_β and T_γ are onset temperatures of each kind of constraints.

Table 1
Glass transition temperature in each composition R [16].

R	*T_g (K)*
0	533
0.05	570
0.1	616
0.15	668
0.2	708
0.2	706
0.3	757
0.3	762
0.4	769
0.5	773
0.6	756
0.7	741
0.8	730
0.9	714
1	694
1.2	651
1.5	602

- D^{4*}: The fraction of D^4 as network-forming species.
- B^{3*}: Three-coordinated boron bonded to three or two bridging oxygen B^3, D^3, T^3 and M^3.
- O^B: Bridging oxygen in each superstructural groups.
- Li^{NB}: Cluster-forming lithium. One Li^{NB} is located by M^3, *loose* N^4 and P^3. And 1.5 Li^{NB} are in O^3.

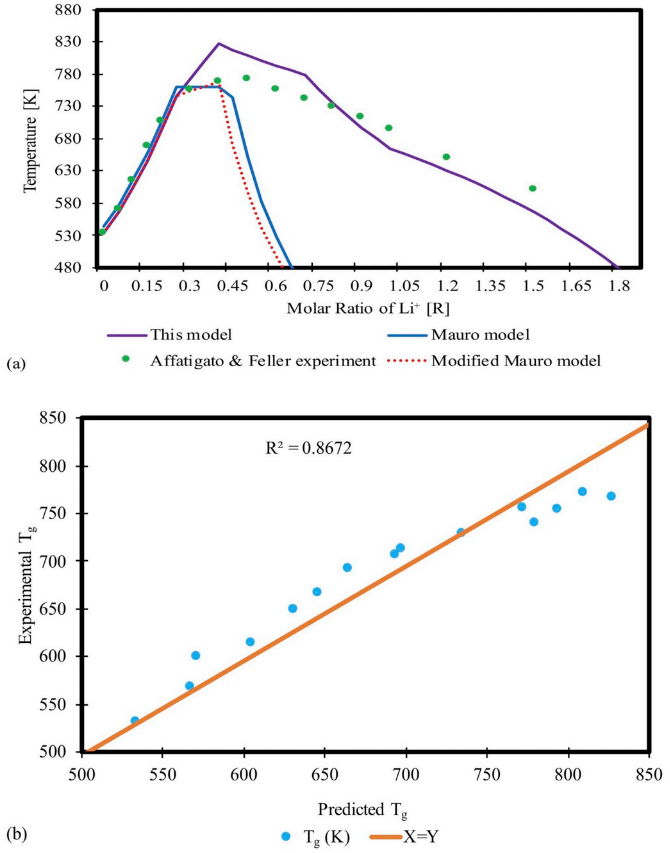

Fig. 5. Calculated glass transition temperature (T_g) by TCT and the plotting of measured T_gs. In (a), This model (purple line) is calculated from Eq. (12), the Mauro model (blue line) is the original work proposed by Mauro et al. in 2009 [5], the Modified Mauro model (red dots) is calculated but without the assumption of μ constraints and Affatigato and Feller experiment (green dots) are measured T_g done by Affatigato and Feller [16]. (b) is the comparison plot of this model and experimental T_g. (For interpretation of the references to colour in this figure legend, the reader is referred to the web version of this article.)

Table 2
Number of constraints in each superstructural groups.

	α	μ	β	γ	Total number of atoms
Loose N^4	4	2	5	2	3
T^4	4	0	5	2	3
D^4	4	0	4.5	2	3
B^3	3	0	3	1.5	2.5
T^3	3	0	3	1.5	2.5
D^3	3	0	3	1.5	2.5
M^3	2	2	3	2	2.5
P^3	0	2	0	2.5	3.5
O^3	0	3	0	3	4

Loose N^4 is four-coordinated boron that does not contribute to the formation of a superstructural group, and it has a negative charge due to the additional electron needed in creating sp^3 hybridization [1]. We suggest that lithium cations can't form ionic bonds with T^4 and D^4, because the charge is conserved as a superstructural group as a whole (see Figs. 2(a) and (b)). Thus, the ion-dipole interaction would be too weak to consider as an ionic bond to be μ constraint between lithium cation and boron tetrahedra. As a result, M^3, *loose* N^4, P^3 and O^3 are chosen to be the superstructural groups which have the capability to form a network with Li^{NB}. To determine the fraction of the five network-forming species, we sum all five network forming species as Ω (see Eq. (8)) using the fraction of superstructural groups (see Fig. 1), and find the ratio of each species as shown in Eqs. (9.a)–(9.e) and shown in Fig. 3.

Table 3
Ionic conductivity of Lithium borate glasses of different compositions at room temperature (293 ± 10 K). R values are calculated from given percentages of lithium oxide from literature by using Eq. (1).

Reference	Year	R	Log conductivity at 293 ± 10 K
Murugaraj R.[a]	2007	0.111111111	−8.965861
Muller K. P.[b]	1969	0.148105626	−16.90735
Muller K. P.[b]	1969	0.176470588	−14.88363
Muller K. P.[b]	1969	0.209189843	−14.22816
Muller K. P.[b]	1969	0.234567901	−14.1806
Muller K. P.[b]	1969	0.25	−13.34685
Muller K. P.[b]	1969	0.283697047	−13.05737
Muller K. P.[b]	1969	0.298701299	−12.68612
Muller K. P.[b]	1969	0.317523057	−12.70562
Muller K. P.[b]	1969	0.333333333	−11.93165
Muller K. P.[b]	1969	0.35501355	−11.01913
Muller K. P.[b]	1969	0.379310345	−10.10824
Muller K. P.[b]	1969	0.400560224	−9.478637
Muller K. P.[b]	1969	0.418439716	−8.954353
Murugaraj R.[a]	2007	0.428571429	−9.758375
Muller K. P.[b]	1969	0.443001443	−7.520871
Muller K. P.[b]	1969	0.47275405	−6.627063
Muller K. P.[b]	1969	0.497005988	−6.119829
Muller K. P.[b]	1969	0.53609831	−5.51017
Muller K. P.[b]	1969	0.615508885	−5.01529
Tatsumisago M.[c]	1986	0.666666667	−8.357701
Muller K. P.[b]	1969	0.683501684	−4.732253
Muller K. P.[b]	1969	0.736111111	−4.589863
Muller K. P.[b]	1969	0.814882033	−4.444539
Muller K. P.[b]	1969	0.912045889	−4.3443
Chowdari B.V.R.[d]	1996	1	−7.655376
Tatsumisago M.[c]	1986	1.5	−6.513937
Yamashita M.[e]	1990	1.817695125	−6.751832

[a] Reference [17].
[b] Reference [18].
[c] Reference [19].
[d] Reference [20].
[e] Reference [21].

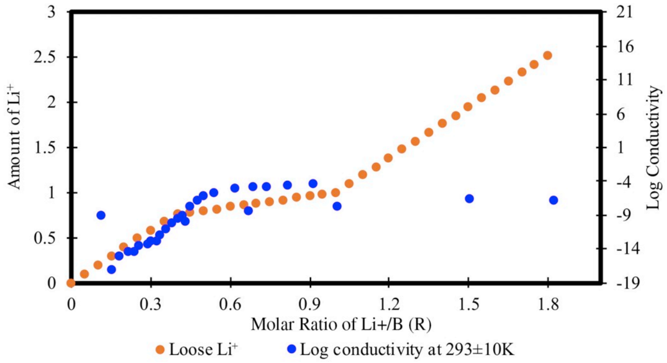

Fig. 6. Orange dots represent the amount of loose Li$^+$ in each composition R and blue dots represent ionic conductivity of lithium ions in each composition R at room temperature 293 ± 10 K. The total amount of lithium ions is given by 2R (Eq. (13)). The list of data and references is in Table 3. (For interpretation of the references to colour in this figure legend, the reader is referred to the web version of this article.)

$$\Omega = Loose\ N^4 + T^4 + D^4 + D^3 + B^3 + T^3 + M^3 + 2(T^4 + D^4 + Loose\ N^4) + 1.5(B^3 + D^3 + T^3) + M^3 + M^3 + Loose\ N^4 + P^3 + 1.5O^3, \tag{8}$$

$$B^{4*} = \frac{Loose\ N^4 + T^4}{\Omega}, \tag{9.a}$$

$$D^{4*} = \frac{D^4}{\Omega}, \tag{9.b}$$

$$B^{3*} = \frac{B^3 + T^3 + D^3 + M^3}{\Omega}, \tag{9.c}$$

$$O^B = \frac{2(T^4 + D^4 + Loose\ N^4) + 1.5(B^3 + D^3 + T^3) + M^3}{\Omega}, \tag{9.d}$$

$$Li^{NB} = \frac{Loose\ N^4 + M^3 + P^3 + 1.5O^3}{\Omega}. \tag{9.e}$$

Using sections II to III, Eq. (4) can be rewritten as

$$n[T_g(R), R] = 2N(O^B) + 5N(B^{4*}) + 4.5N(D^{4*}) + 3N(B^{3*}) + 2N(Li^{NB}), \tag{10}$$

by combining Eqs. (2)–(10), the corresponding low frequency mode can be given by

$$f[T_g(R), R] = 3 - n[T_g(R), R], \tag{11}$$

which is plotted in Fig. 4. By combining Eqs. (3) and (11), the T_g can be computed as shown in Eq. (12),

$$T_g(R) = \frac{f[T_g(0), 0]}{f[T_g(R), R]} T_g(0), \tag{12}$$

where $T_g(0) = 533K$ from the literature shown in Table 1 [16].

4. Results

$T_g(R)$ is calculated by using Eq. (12) and compared to the experimental data which was compiled as shown in Table 1 [16], and plots are shown in Fig. 5(a). In Fig. 5(a), T_g is calculated under the assumption of the lithium clustering effect. Mauro model represents the original Mauro model published in 2009 [5]. The modified Mauro model takes into account the assumption of overcounted β constraints in the diborate ring. Table 2 shows the number of each constraints in each of the superstructural groups. The comparison plots between the T_g calculated here and the experimental T_g [16] are given in Fig. 5(b). R^2 was found to be 0.8672.

5. Discussion

We have calculated the glass transition temperature (T_g) using TCT [5,13] with the added assumption of overcounted constraints in the diborate ring and the further assumption of alkali constraints. Previously, the onset temperature of the β constraint (T_β) has been assumed from the literature, to be that of the flat region $0.2 \le R \le 0.45$ (shown in Fig. 5(a)), this was found to 760 K [5,7]. However, although the prediction of T_g is higher than the literature in the region $0.3 \le R \le 0.8$, the experimental T_g and the predicted T_g are correlated to each other (see Fig. 5(a)). This result indicates the existence of the possible overcounted β constraints in the diborate ring.

Alkali constraints have previously been assumed to just be fitting parameters due to alkali additions to rigidity, however, we have shown that they can be correlated with the presence of superstructural groups, which allows us to make an in-depth discussion about the characteristics of modifier ions in the vitreous network. Li^{NB} is the lithium ions which contribute to form a network, in other words Li^{NB} is relatively rigid compared to the other lithium ions. Through this logic, we took the difference between the total number of lithium ions to Li^{NB} and we named this formula unit as *loose Li*$^+$ as shown in below,

$$Loose\ Li^+ = 2R - Li^{NB}, \tag{13}$$

where *2R* represents all lithium ions since each lithium oxide has two lithium ions.

The *loose Li*$^+$ and the experimental data of ionic conductivity at room temperature (293 ± 10 K) [17–21] (see Table 3) are compared in Fig. 6. As can be seen, there is a clear proportionality in the region $0 \le R \le 1$. However, this trend collapses when $R > 1$. There are few experimental data of ionic conductivity at room temperature in the literature for $R \geq 1$ due to the difficulty of forming a vitreous network in high alkali compositions, even using fast cooling procedures such as roller quenching. Although we would assume that there would be some physical affect which makes lithium ions difficult to move in the glassy network rather being constrained by μ constraints (which are ionic interactions), further discussion will occur in the future.

Through these discussions, this model gives evidence for the weak electrolyte model of ionic conductivity [22] in the region $0 \leq R \leq 1$, in which the mobility is a constant and the fraction of ions moving is dynamic, which would relate back to the number of constraints holding the lithium as part of the network.

6. Conclusion

In this study, we have determined the glass transition temperature (T_g) of alkali borates by using TCT and the structural model based on NMR of lithium borate glasses [1]. The possibly overcounted β constraint in the diborate ring and the difference of ions' mobility due to the rigidity of μ constraint have new features in the proposed model. Although, the dynamic movement of lithium cations deviate from the literature in the region $1 < R$, we proposed a model which allows us to deduce a physical origin of ionic conductivity from the topological origin of modifier rigidity.

Acknowledgments

The authors would like to thank the NSF (DMR 1746230) for funding of this research, Dr. Caio Braggatto is acknowledged for useful discussions.

Declaration of interests

The authors declare that they have no known competing financial interests or personal relationships that could have appeared to influence the work reported in this paper.

The authors declare the following financial interests/personal relationships which may be considered as potential competing interests.

References

[1] P.J. Bray, et al., B10 NMR studies of the structure of borate glasses, J. Non-Cryst. Solids 39 (1980) 93–98.
[2] A. Vegiri, C.P.E. Varsamis, Clustering and percolation in lithium borate glasses, J. Chem. Phys. 120 (2004) 7689–7695.
[3] Krogh-Moe, Interpretation of infrared spectra of boron oxide and alkali borate glasses, Phys. Chem. Glasses 6 (1965) 46–54.
[4] E.I. Kamitsos, G.D. Chryssikos, Borate glass structure by Raman and infrared spectroscopies, J. Mol. Struct. 247 (1991) 1–16.
[5] J.C. Mauro, P.K. Gupta, R.J. Loucks, Composition dependence of glass transition temperature and fragility. II. A topological model of alkali borate liquids, J. Chem. Phys. 130 (2009) 234503.
[6] P.K. Gupta, The random-pair model of four-coordinated borons in alkali-borate glasses, Proc. Int. Congr. Glas. New Delhi, India 11 (1986).
[7] M.S. Bødker, J.C. Mauro, R.E. Youngman, M.M. Smedskjaer, Statistical mechanical modeling of borate glass structure and topology: prediction of superstructural units and glass transition temperature, J. Phys. Chem. B 123 (2019) 1206–1213.
[8] S.A. Feller, W.J. Dell, P.J. Bray, B10 NMR studies of lithium borate glasses, J. Non-Cryst. Solids 51 (1982) 21–30.
[9] S. Goyal, J.C. Mauro, Statistical mechanical model of bonding in mixed modifier glasses, J. Am. Ceram. Soc. 101 (2018) 1906–1915.
[10] P.K. Gupta, J.C. Mauro, Composition dependence of glass transition temperature and fragility. I. A topological model incorporating temperature-dependent constraints, J. Chem. Phys. 130 (2009) 094503.
[11] G.G. Naumis, Energy landscape and rigidity, Phys. Rev. E – Stat. Nonlinear Soft Matter Phys. 71 (2005) 26114.
[12] G.G. Naumis, Glass transition phenomenology and flexibility: an approach using the energy landscape formalism, J. Non-Cryst. Solids 352 (2006) 4865–4870.
[13] M.M. Smedskjaer, J.C. Mauro, S. Sen, Y. Yue, Quantitative design of glassy materials using temperature-dependent constraint theory, Chem. Mater. 22 (2010) 5358–5365.
[14] J.C. Mauro, Topological constraint theory of glass, Am. Ceram. Soc. Bull. 90 (2011) 31–37.
[15] M. Thorpe, Continous deformations in random networks, J. Non-Cryst. Solids 57 (1983) 355–370.
[16] M. Affatigato, et al., The glass transition temperature of lithium and lithium-sodium borate glasses over wide range of composition, Phys. Chem. Glasses 31 (1990) 19–24.
[17] R. Murugaraj, Ac conductivity and its scaling behavior in borate and bismuthate glasses, J. Mater. Sci. 42 (2007) 10065–10073.
[18] K.P. Muller, Strktur und Eigenschaften von Glasern und glasbildenden Schmelzen, Glas. Ber. 42 (1969) 83–89.
[19] M. Tatsumisago, T. Minami, Lithium ion conducting glasses prepared by rapid quenching, Mater. Chem. Phys. 18 (1987) 1–17.
[20] Z. Rong, B.V.R. Chowdari, The role of Bi_2O_3 as a network modifier and a network former in $xBi_2O_3.(1-x)LiBO_2$ glass system, Solid State Ionics 90 (1996) 151–160.
[21] M. Yamashita, R. Terai, Ionic conductivity of Li_2O-B_2O_3-Li_2SO_4 glasses, Glas. Berichte-Glass Sci. Technol. 63 (1990) 13–17.
[22] D. Ravaine, Ionic transport properties in glasses, J. Non-Cryst. Solids 73 (1985) 287–303.